Angewandte Chemie
Eine Zeitschrift der Gesellschaft Deutscher Chemiker

Supporting Information

69451 Weinheim, Germany

Ag_7Au_6: A 13-Atom Alloy Quantum Cluster**

*Thumu Udayabhaskararao, Yan Sun, Nirmal Goswami, Samir K. Pal, K. Balasubramanian, and Thalappil Pradeep**

anie_201107696_sm_miscellaneous_information.pdf

Table of contents

S1. Supporting information 1

Experimental Section

Synthesis of $Ag_{7,8}$: About 85 mg of $AgNO_3$, dissolved in 1.7 mL water, was added to 448.9 mg of H_2MSA in 100 mL methanol under ice-cold conditions with vigorous stirring. Silver was reduced to the zero-valent state by slow addition of freshly prepared aqueous $NaBH_4$ solution (0.2 M, 25 mL). The reaction mixture was stirred for 1 h. The resulting precipitate was collected and repeatedly washed with methanol by centrifugal precipitation. Finally, the Ag@(H_2MSA) precipitate was dried and collected as a dark brown powder. Interfacial etching was performed in an aqueous/organic biphasic system. Ag@(H_2MSA) (100 mg in 100 mL H_2O) was dispersed in the aqueous phase. An aqueous solution of the as-synthesized Ag@(H_2MSA) nanoparticles was added to an excess of H_2MSA in toluene (1/2 water/toluene ratio). A weight ratio of 1:3 was used (Ag@(H_2MSA):H_2MSA). The resulting mixture was stirred for 48 h at room temperature (ca. 300 K). Initiation of interfacial etching is indicated by the appearance of a blue layer at the interface after 0.5–1 h. As the reaction proceeds, the color of the aqueous phase changes from reddish brown to yellow, and finally to orange. After centrifugation, thiolate got precipitated and gives a reddish brown solution which contains Ag_8, Ag_7, smaller amounts of thiolate and unbound H_2MSA. This solution is mentioned as crude $Ag_{7,8}$ cluster solution. For further purification the solution was concentrated using freeze dry. The concentrated sample was centrifuged at 18,000 rpm, 278 K for 20 min to remove of thiolates. By the addition of methanol to supernatant, cluster product was precipitated from it and the precipitate was repeatedly washed with 90% methanol to remove excess H_2MSA. The final precipitate contains both clusters and free from thiolates and H_2MSA.

Ag_7Au_6 clusters were prepared as mentioned in the main text.

Ligand exchange reactions: Exchange reaction was done with phenylethanethiol (PET), hexanethiol (HT) and octanethiol (OT). 0.01M of these thiols were taken in 2.0 mL of toluene on top of 3.0 mL (3.3 mg/mL) of $Ag7Au6(H_2MSA)_{10}$ cluster solution. The mixture was gently stirred for 3 hours at 273 K. Exchange can be observed directly by visible color change of the toluene phase form colorless to reddish yellow. This was subjected to solvent evaporation to yield a paste-like material, which was washed with water several times and the final precipitate was soluble in toluene. Analytical and computational methods are described in S1.

Synthesis of Ag_{QC}@SG: Ag@H_2MSA nanoparticles and glutathione were taken (weight ratio of 1:3) in aqueous/toluene biphasic system. The resulting mixture was stirred for 48 h at room temperature (~300 K). As the reaction proceeds, the reddish brown color of the aqueous phase gradually disappears and finally it converts to orange. The separated aqueous phase is freeze dried and was washed with methanol to remove excess GSH. The product in powder form was obtained by solvent evaporation using rotavapor and stored in closed container since it is hygroscopic.

Phase transfer of $Ag_7Au_6(H_2MSA)_{10}$: 10 mg of alloy clusters was dissolved in 50 mL of distilled water. 5 mL of 3 mM TOABr [tetraoctylammonium bromide $\{CH_3(CH_2)_7\}_4N$ Br)] in toluene was added to make an immiscible layer above the water phase. Toluene got colored upon stirring the mixture for 2 min, indicating the transfer of cluster from aqueous to organic phase. Phase transfer occurred due to the electrostatic interaction of anionic carboxylic group of MSA to quaternary nitrogen group of TOA^+.

Purification by polyacrylamide gel electrophoresis (PAGE): PAGE separation of the clusters was performed as per the procedure given below.

A gel electrophoresis unit with 1 mm thick spacer (Bio-rad, Mini-protein Tetra cell) was used to process the PAGE. The total contents of the acrylamide monomers were 28% (bis(acrylamide:acrylamide) = 7:93) and 3% (bis(acrylamide:acrylamide) = 6:94) for the separation and condensation gels, respectively. The eluting buffer

consisted of 192 mM glycine and 25 mM tris(hydroxymethylamine). The crude mixture of Ag@(H_2MSA) clusters, as a reddish brown powder, obtained in the reaction was dissolved in 5% (v/v) glycerol-water solution (1.0 mL) at a concentration of 60 mg/mL. The sample solution (1.0 mL) was loaded onto a 1 mm gel and eluted for 4 h at a constant voltage of 120 V to achieve separation shown in Figure 1. During the gel electrophoresis, PAGE setup was kept at ice cold temperature. The gel fractions containing the cluster were cut out, ground, and dipped in ice cold distilled water (2 mL) for 10 min. Subsequently, the solutions were centrifuged at 20,000 rpm for 5 min at -263 K, followed by filtering with filter paper having 0.22 μm pores to remove the gel lumps suspended in the solution. The samples were freeze dried to get reddish yellow powders. Same procedure was used to separate Ag_8 cluster from $Ag_{7,8}$.

We also performed high resolution electrophoresis using increased contents of acrylamide monomers of 35% for the separation gel. However, we did not observe any additional bands.

Analytical procedures

A. UV-vis spectroscopy

Perkin Elmer Lambda 25 UV-vis spectrometer was used for the measurements. Spectra were typically measured in the range of 190-1100 nm. The experimentally obtained spectral data, *I*(?), which are functions of wavelength, were converted to the energy dependent data, *I*(*E*), according to the following relation, *I*(*E*) = *I*(?) / (?*E*/? ?) a *I*(?) × ?^{2} where ?*E*/? ? represents the Jacobian factor.

B. Fourier-transform infrared (FT-IR) spectra

FT-IR spectra were measured with a Perkin Elmer Spectrum One instrument. KBr crystals were used as the matrix for sample preparation.

C. Luminescence spectroscopy

Luminescence measurements were carried out using HORIBA JOBIN VYON Nano Log instrument. The band pass for excitation and emission was set as 3 nm.

D. Transmission electron microscopy (TEM)

TEM images were collected using a JEOL 3010 microscope. A diluted solution was spotted on carbon coated copper grid and was dried in laboratory ambience. Images were collected at 200 keV, to reduce beam induced damage of the clusters. Our earlier studies had shown that small clusters are highly sensitive to electron beam and they coalesce to yield nanoparticles on the grid.

E. Electrospray ionization (ESI) mass spectrometry (MS)

The ESI MS measurements were done in the negative mode using an MDX Sciex 3200 QTRAP MS/MS instrument having a mass range of m/z 50-2000. A 50% (v/v) methanol/toluene cluster solution (0.1 mg/mL) was electrosprayed through a stainless steel needle biased at ca. -3 kV. The solution was delivered by a syringe pump at a typical flow rate of 8 µL/min. Under an optimized capillary temperature (ca. 353 K), evaporation of the solvents from the droplets proceeds efficiently so that only the desolvated cluster ions in the intact form were formed at maximum yield. We observed dissociation of the intact clusters into small fragments, at higher capillary temperatures.

G. SEM and EDAX analyses

Scanning electron microscopic (SEM) and energy dispersive X-ray (EDAX) analyses were done in a FEI QUANTA-200 SEM. For measurements, samples were drop-casted on an indium tin oxide coated conducting glass and dried in vacuum.

H. X-ray photoelectron spectroscopy

The photoelectron spectra of the samples were obtained using an ESCA probe/TPD of Omicron Nanotechnology. Sample in water was spotted on a Mo plate and allowed to dry in vacuum. The size of the analyzed area was about 3 mm^2. In view of the sensitivity of the sample, surface cleaning was not attempted. Al K_a radiation was used for excitation; a 180° hemispherical analyzer and a seven-channel detector were employed. The spectrometer was operated in the constant analyzer energy mode. Survey and high-resolution spectra were collected using pass energies of 50 and 20 eV, respectively. The pressure in the analyzer chamber was in the low 10^{-10} mbar range during spectrum collection. Binding energies of the core levels were calibrated with C 1s BE, set at 284.7 eV.

I. Luminescence imaging

A Witec GmbH confocal Raman spectrometer, equipped with a Nd:YAG laser frequency doubled laser at 532 nm was used as the excitation source to collect the luminescence images. The laser was focused onto the sample using a 100X objective with the signal collected in a back scattering geometry. The signal, after passing through a super notch filter, was dispersed using a 150 grooves/mm grating onto a Peltier-cooled charge coupled device (CCD), which served as the detector. The sample mounted on a piezo stage was scanned with signals collected at every step. For the images displayed, the scan area was divided into 100X100 pixels for spectral image acquisition. Spectral intensities acquired over a predefined area were automatically compared to generate color-coded images. In the images, regions coded yellow are regions with maximum fluorescence intensities and regions shown in black are with minimum signal intensities.

J. Quantum yield

The quantum yield (QY) of the cluster was measured using rhodamine 6G (in water) as a reference.

K. Computational methods

The structure for $Ag_7Au_6(SR)_{10}$ was determined theoretically by performing density functional calculations with the Gaussian 09 software [1] using Perdew-Burke-Ernzerhof (PBE) exchange-correlation (XC) functional,[2] together with relativistic effective core potentials (RECP) that kept the outer valence $4d^{10}5s^1$ shells of silver atom, $2s^22p^2$ for carbon atom, and $3s^2\ 3p^4$ for sulfur atom, replacing the rest electrons by RECP.[3] After obtaining the optimized ground state structures of Ag_7Au_6 core by global optimization method Taboo Search in Descriptor Space (TSDS),[4] we passivated 10 methanethiolate (SCH_3) ligands on the optimized Ag_7Au_6 core and re-optimized these $Ag_7Au_6(SCH_3)_{10}$ structures, followed by single point calculations for triplet states of $Ag_7Au_6(SCH_3)_{10}$ based on the structures of the ground states. The simulated absorption spectra of this structure obtained by time-dependent density functional theory (TDDFT).

L. Life time measurements

Picosecond resolved photoluminescence transients of $Ag_7Au_6(SR)_{10}$ cluster were measured using a commercially available spectrophotometer (LifeSpec-ps, Edinburgh Instruments, UK) with a 409 nm excitation laser having

instrument response function (IRF) of 60 ps. The picosecond-resolved ?uorescence transients have been fitted with tri-exponential function, $\sum_{i=1}^{3} A_i \exp(-t/t_i)$, where, A's are weight percentages of the decay components with time constants of t_i. The relative change in the overall excited state lifetime is expressed by the equation $t = \sum_{i=1}^{3} A_i t_i$, when $\sum_{i=1}^{3} A_i = 1$. It has to be noted that with our time resolved instrument after deconvolution, we can resolve at least one fourth of the instrument response time constants.

References:

[1] Gaussian 09, Revision A.1, Frisch, M. J.et al.
[2] Perdew, J. P.; Burke, K.; Ernzerhof, M.; *Phys. Rev. Lett.* **1996,** *77*, 3865; **1997**, *78*, 1396 (E).
[3] Ross, R.B.; Powers, J. M.; Atashroo, T.; Ermler, W.C.; LaJohn, L. A.; Christainsen, P. A.; *J. Chem. Phys.* **1990**, *93*, 6654.
[4] Cheng, J.; Fournier, R.; *Theor. Chem. Acc.* **2004**, *112*, 7.

S2. Supporting information 2

Confirmation of AgCl from SEM/EDAX and XRD

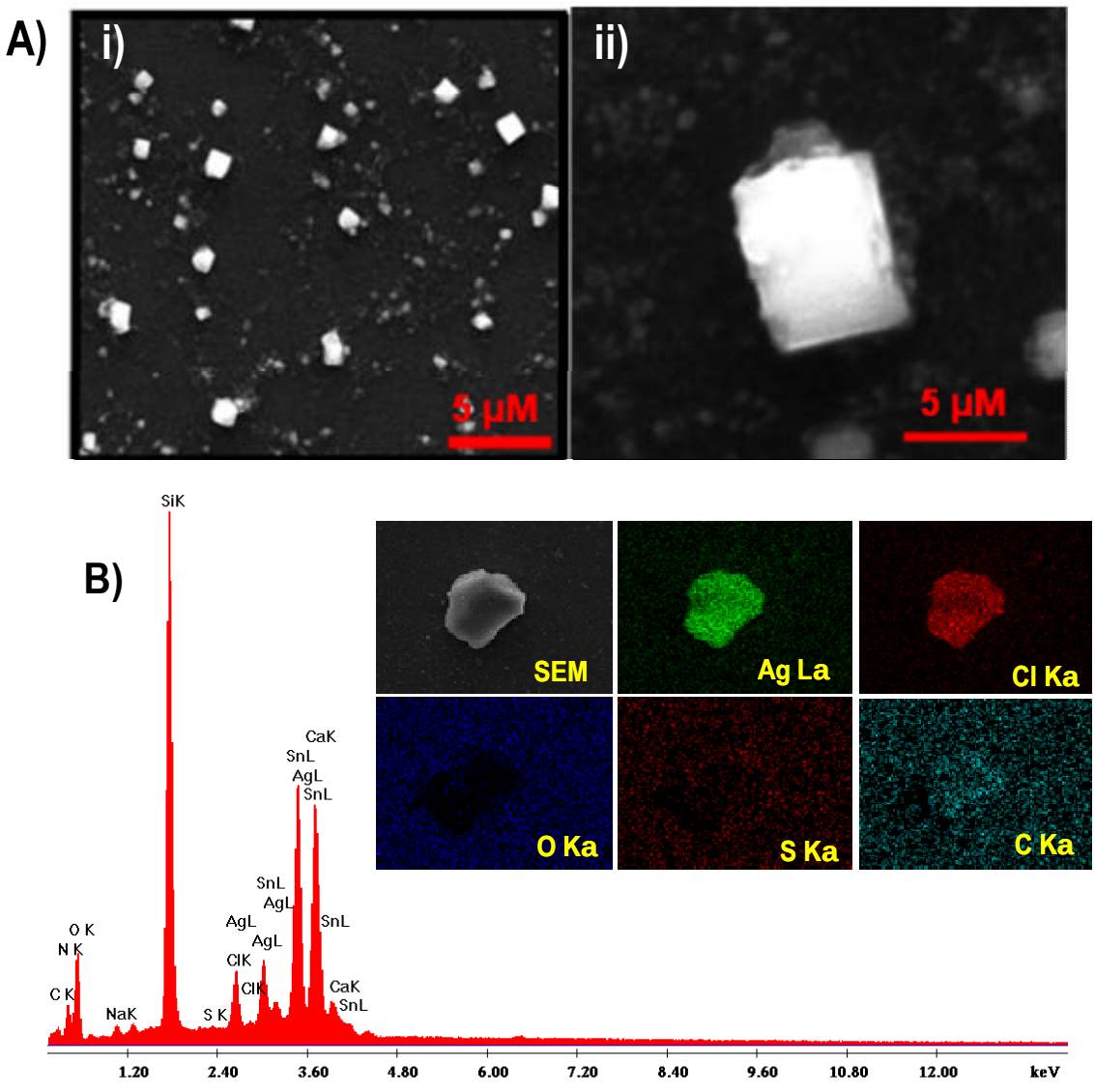

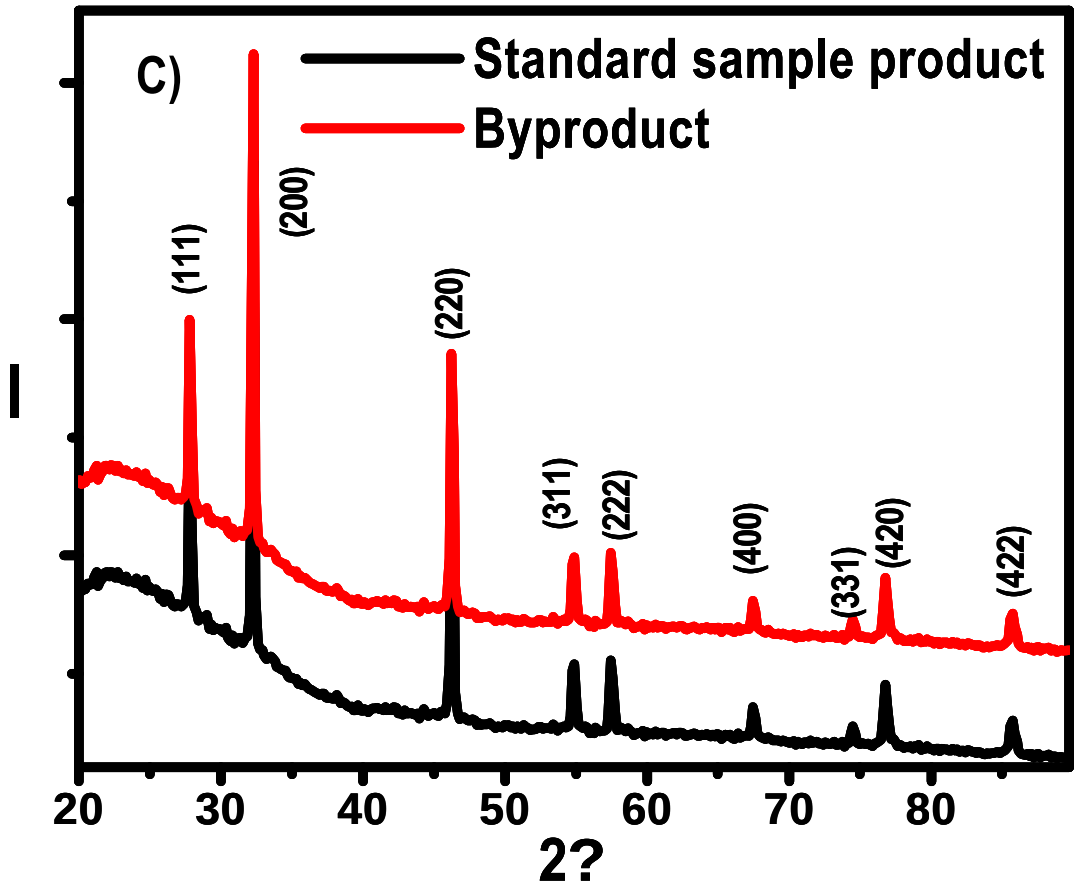

Figure S1.

A) I) SEM image of the byproduct during the synthesis of alloy QCs, showing the presence of 1-5 μM sized AgCl crystals, one such crystal is in closer view is shown in image II).

B) EDAX spectrum and elemental images of the byproduct crystal (I) EDAX spectrum of the byproduct. II) SEM image of the crystal and EDAX maps using III) Ag $\mathbf{M}_a$, (IV) Cl $\mathbf{K}_a$, (V) O $\mathbf{K}_a$ (VI) S $\mathbf{K}_a$, and (VII) C $\mathbf{K}_a$ are shown. Sn $\mathbf{L}_a$ and In $\mathbf{L}_a$ lines are due to the indium tin oxide substrate used. Ag:Cl atomic ratio measured is almost 1:1, which proves the presence of AgCl.

C) XRD patterns of the byproduct obtained during the reaction, is compared with the standard AgCl XRD patterns. Lattice planes are assigned based on JCPDS file no 85-1355. The formation of AgCl confirms that silver atoms from the cluster core are leaching out. Note that Cl^- is coming from the $HAuCl_4$ precursor used in the reaction.

S3. Supporting information 3

Comparison of crude and PAGE separated clusters

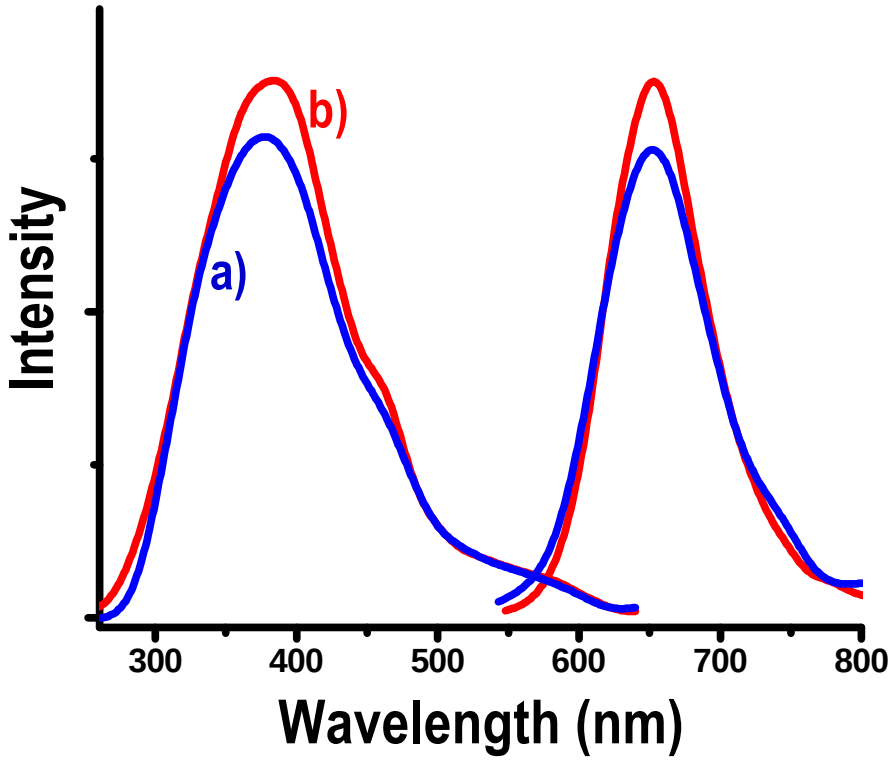

Figure S2. Luminescence spectra of the cluster in water collected at 300 K using the same concentrations. Comparison of the luminescence spectra of (a) as-synthesized cluster (before PAGE) and b) purified cluster (after PAGE).

S4. Supporting information 4

TEM, effect of electron beam irradiation images

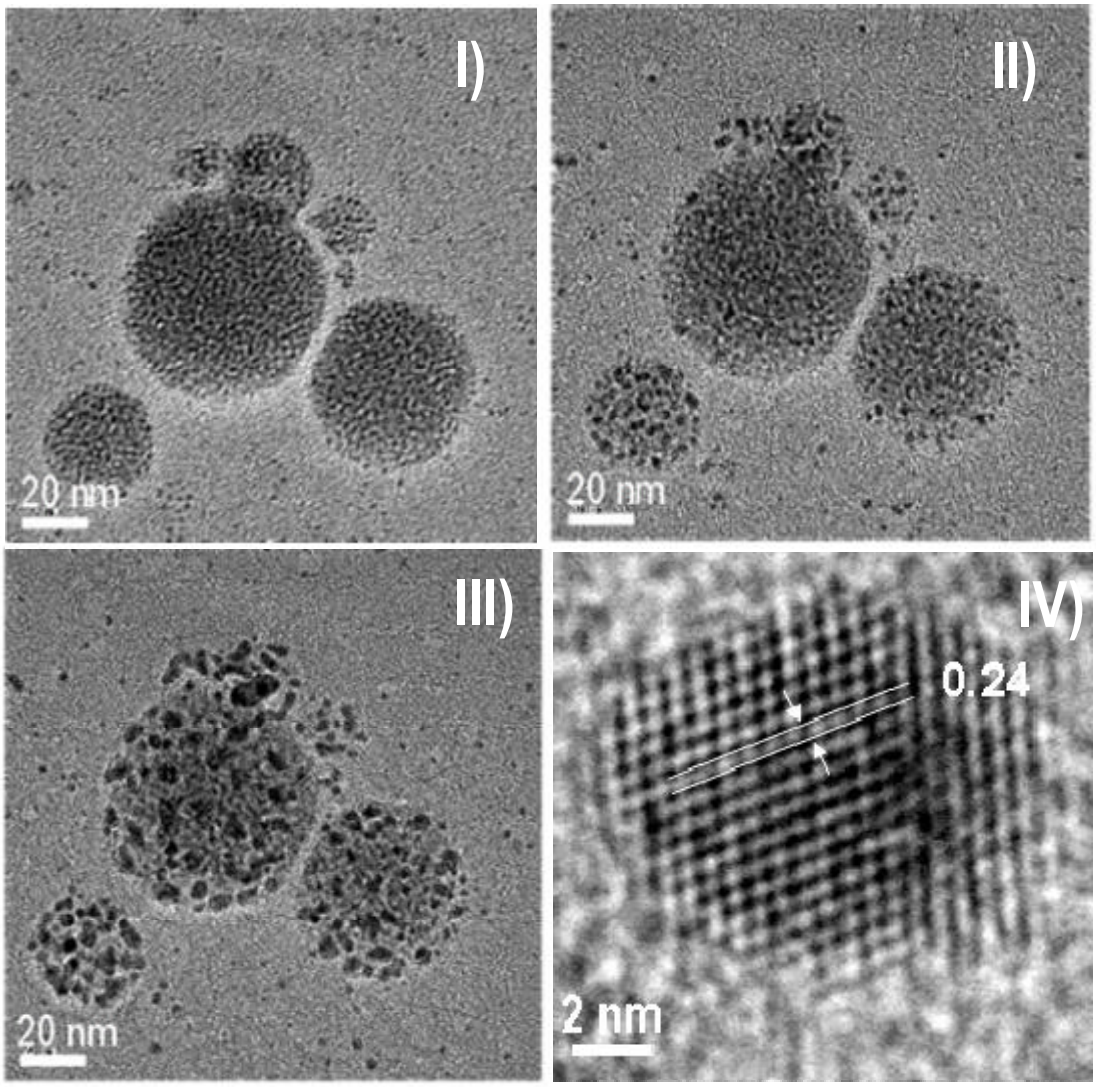

Figure S3. TEM image of Ag_7Au_6 cluster aggregates (I), which upon continuous electron beam irradiation (II) and (III) coalesce to form larger nanoparticles. The same regions of the grid are shown in the images. Image (I) is at the start of the irradiation showing small clusters, image (II) is after 10 min and image and (III) is after 20 min. The contrast from the clusters is poor unlike in the case of nanoparticles. Image (IV) is of one grown particle showing the lattice (shown by lines).

S5. Supporting information 5

XPS

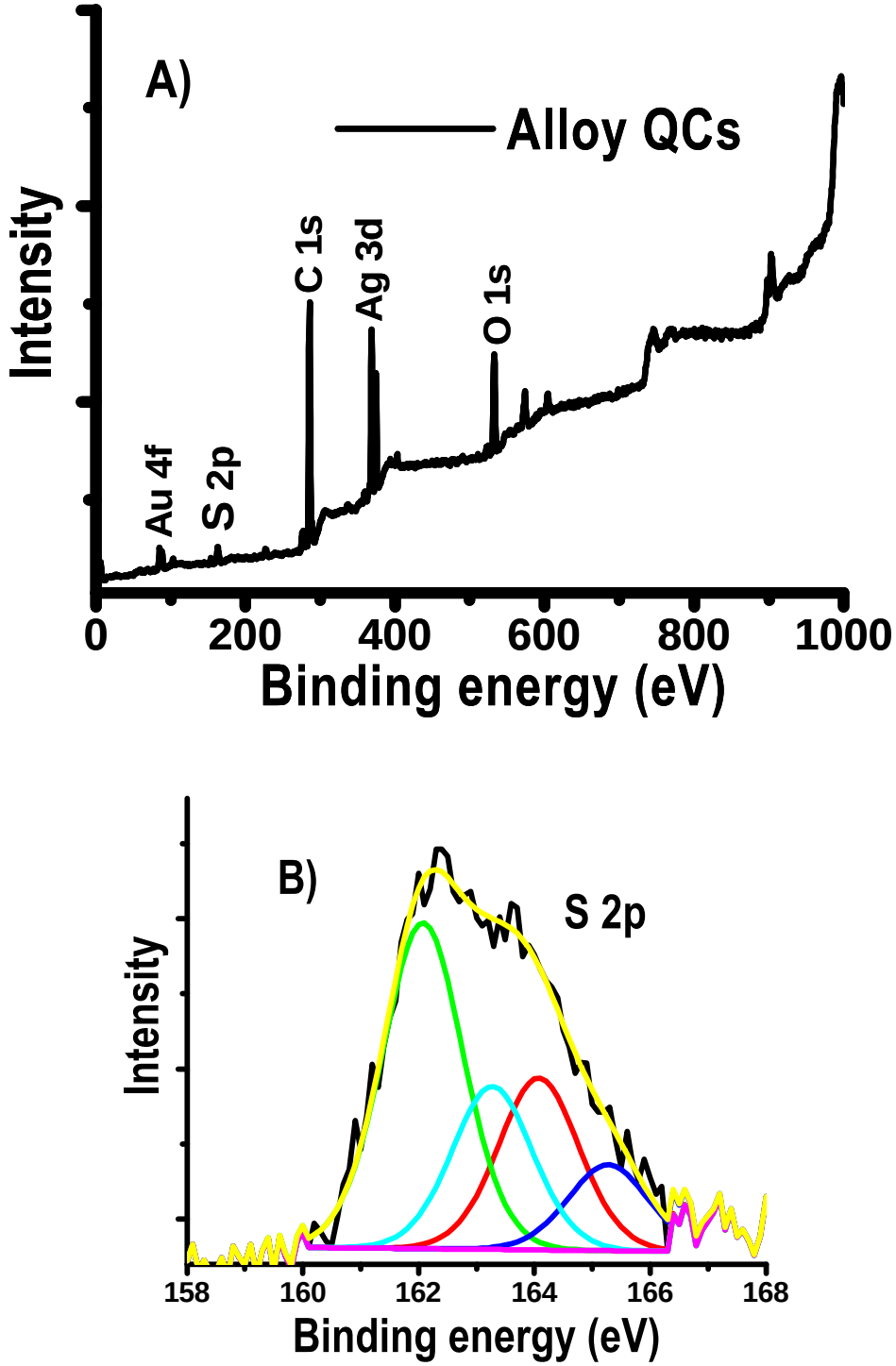

Figure S4. (A) XPS survey spectrum of the as-synthesized alloy QCs. (B) Expanded S 2p core level region. The Ag:Au:S atomic ratio is 1:0.84:1.40 whereas the expected value is 1:0.86:1.43. The S $2p_{3/2}$ exhibits a thiolate position of 162.0 eV and an additional S $2p_{3/2}$ peak at 164.1 eV observed upon peak fitting may be due to other ligand binding sites or X-ray induced damage. Total peak area was considered to get the atomic percentage of sulfur.

S6. Supporting information 6

FT-IR

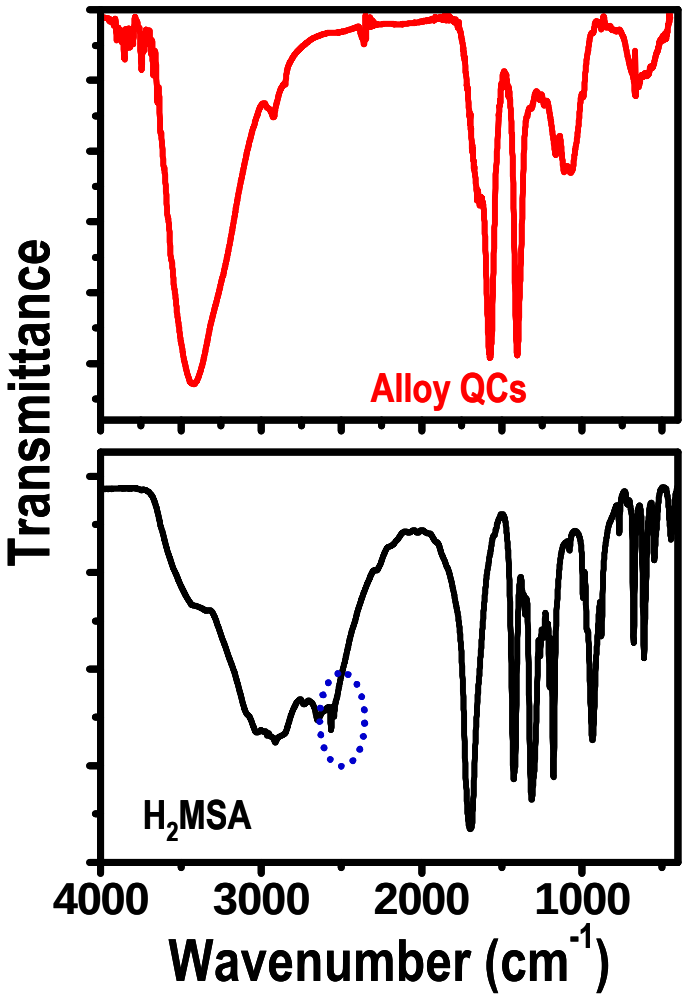

Figure S5. FT-IR spectra of pure H_2MSA, alloy QCs. The -SH stretching feature at 2552 cm^{-1} in H_2MSA is marked by the dotted-circle is absent in the alloy QCs spectrum, in agreement with the XPS. H_2MSA features in the region of 2000-500 cm^{-1} confirm the cluster was protected by H_2MSA. A strong band at 3435 cm^{-1} due to the hydrated water.

S7. Supporting information 7

SEM/EDAX

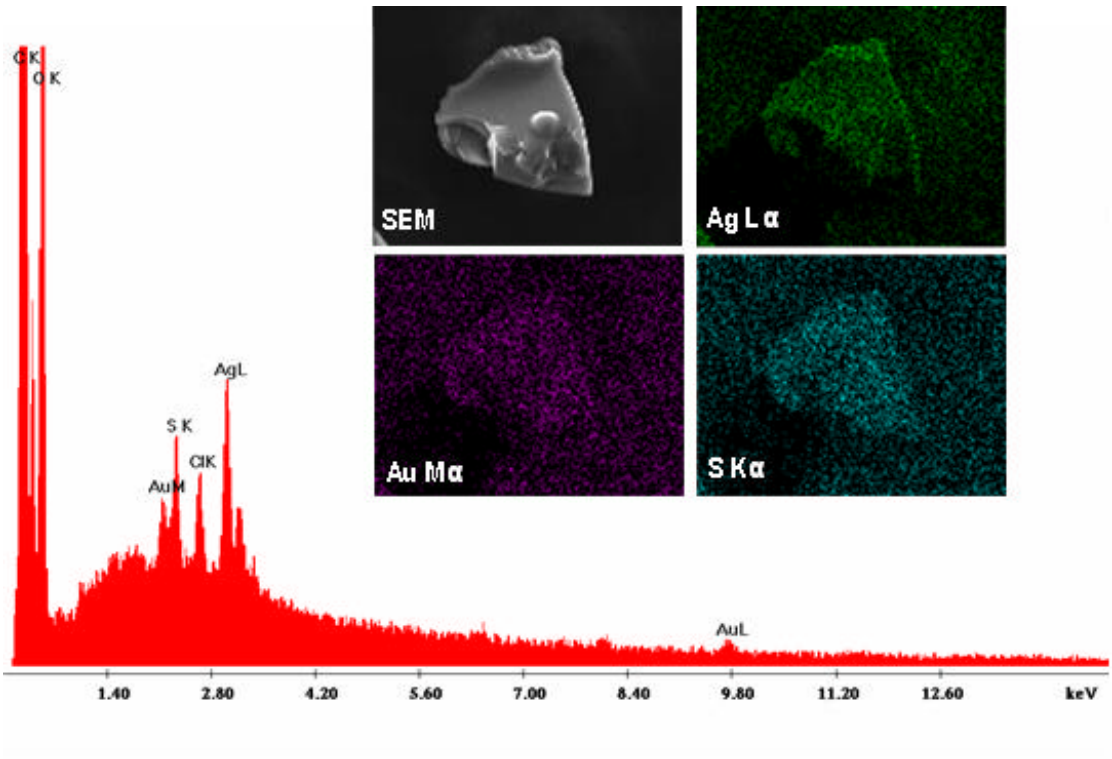

Figure S6. EDAX spectrum collected from alloy QCs. Inset showing the SEM image of the alloy QCs aggregate from which the EDAX spectrum was taken. EDAX maps using Ag $\mathbf{L}_a$, Au $\mathbf{M}_a$, S $\mathbf{K}_a$. Ag:Au:S atomic ratio measured is 1:0.82:1.42, whereas that expected is 1:0.86:1.43.

S8. Supporting information 8

Another structure of the model cluster, $Ag_7Au_6(SCH_3)_{10}$

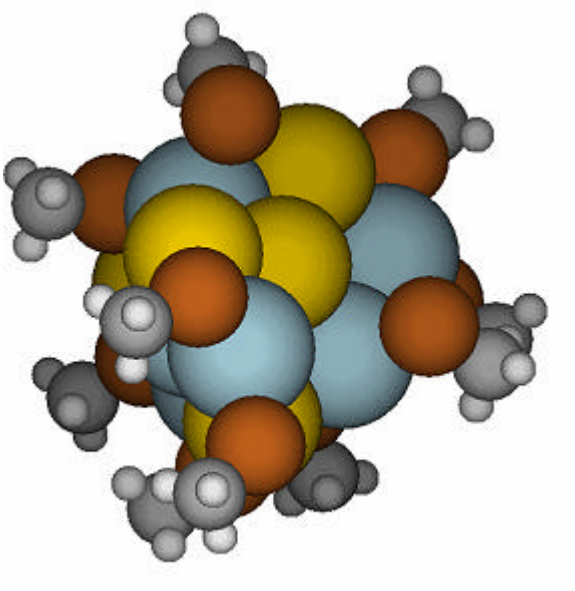

Figure S7. Another possible structure of the model cluster, $Ag_7Au_6(SCH_3)_{10}$. Ag is blue, Au is yellow and S is brown. CH_3 units are also shown.

S9. Supporting information 9

Luminescence of ligand exchanged products

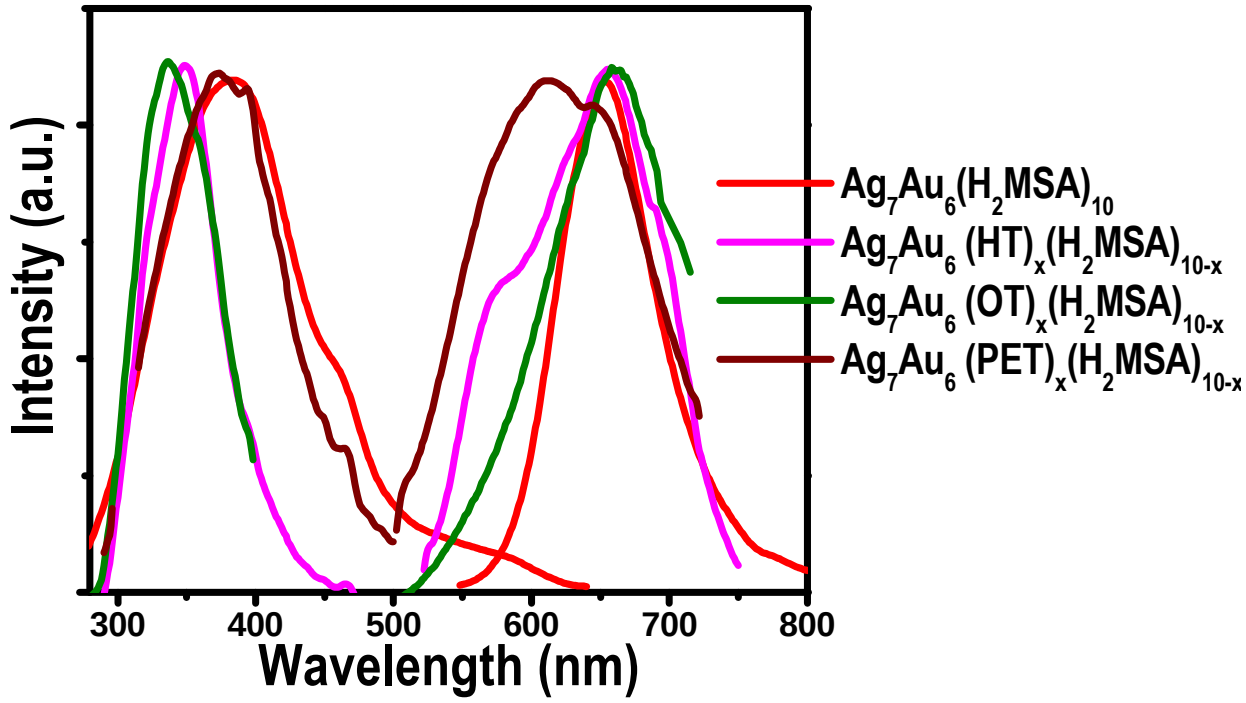

Figure S8. Luminescence spectra of the ligand exchanged cluster solution, excitation at 350±30 nm and emission show a maxima of 650±30 nm for $Ag_7Au_6(H_2MSA)_{10}$, $Ag_7Au_6(HT)_x(H_2MSA)_{10-X,}$ $Ag_7Au_6(OT)_x(H_2MSA)_{10-x}$ and $Ag_7Au_6(PET)_x(H_2MSA)_{10-x}$.

S10. Supporting information 10

ESI MS of $[Ag_7Au_6(HT)_{10}]^{2+}$

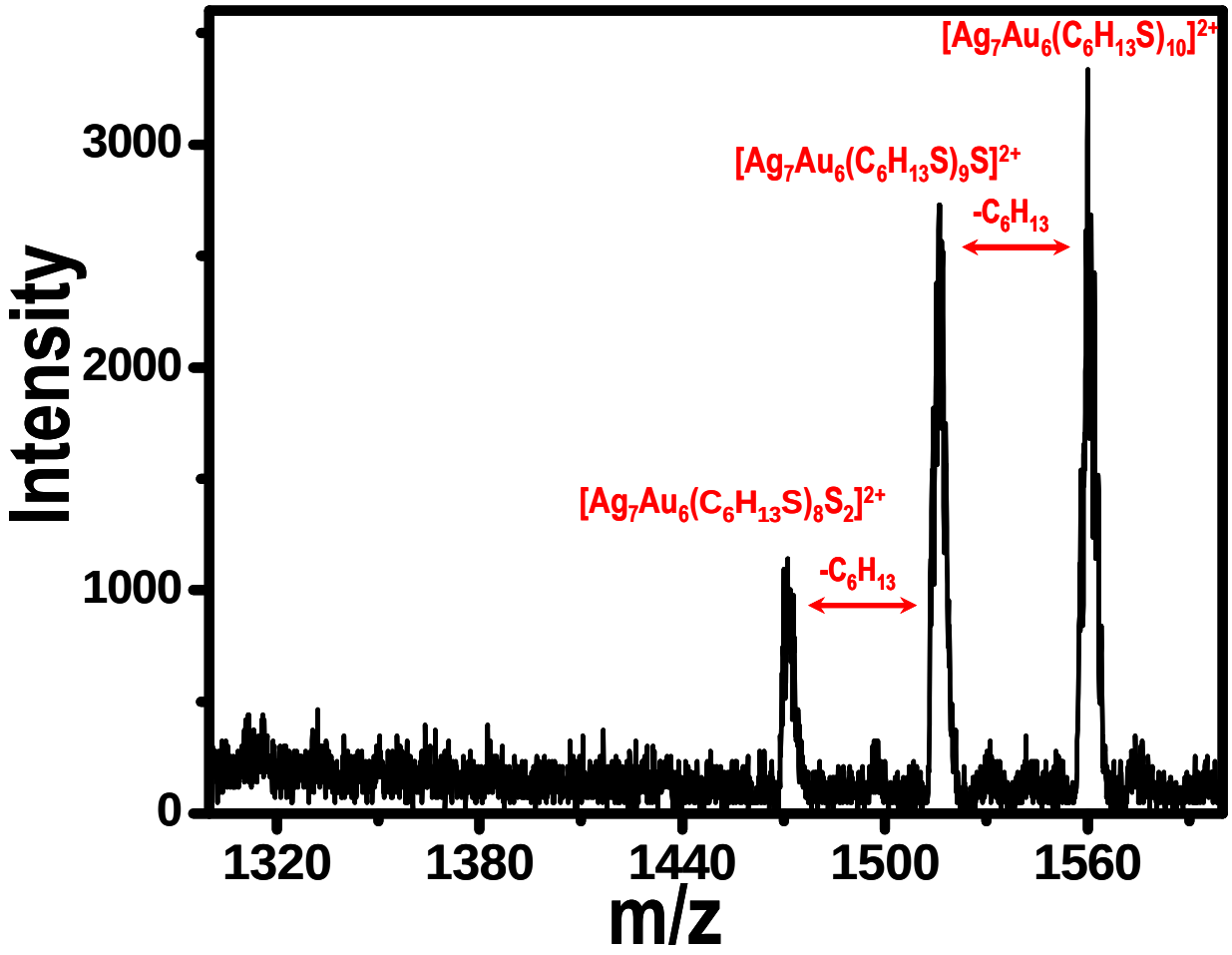

Figure S9. ESI MS of the hexane thiol exchanged cluster in the positive mode in the region of m/z 1300-1600. The ion $[Ag_7Au_6(C_6H_{13}S)_{10}]^{2+}$ and its sequential $-C_6H_{13}$ losses are also seen in the spectrum. The spectrum confirms the presence of ten ligands.

S11. Supporting information 11

Luminescence spectra of $Ag_7Au_6(H_2MSA)_{10}$ before and after phase transfer

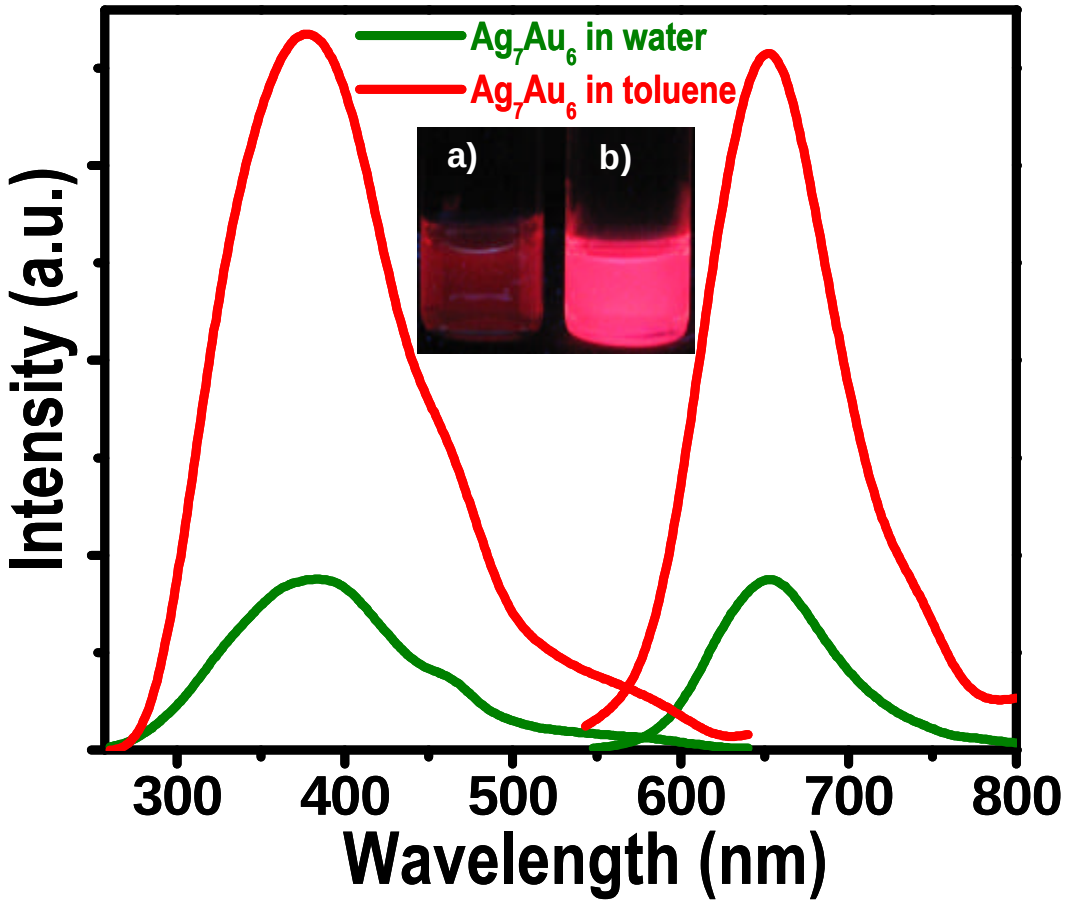

Figure S10. Luminescence spectra of $Ag_7Au_6(H_2MSA)_{10}$ in water and in toluene after phase transfer. Phase transfer increases luminescence emission. Inset shows the photographs of $Ag_7Au_6(H_2MSA)_{10}$ a) before (left) and b) after (right) phase transfer.

S12. Supporting information 12

Lifetime measurements

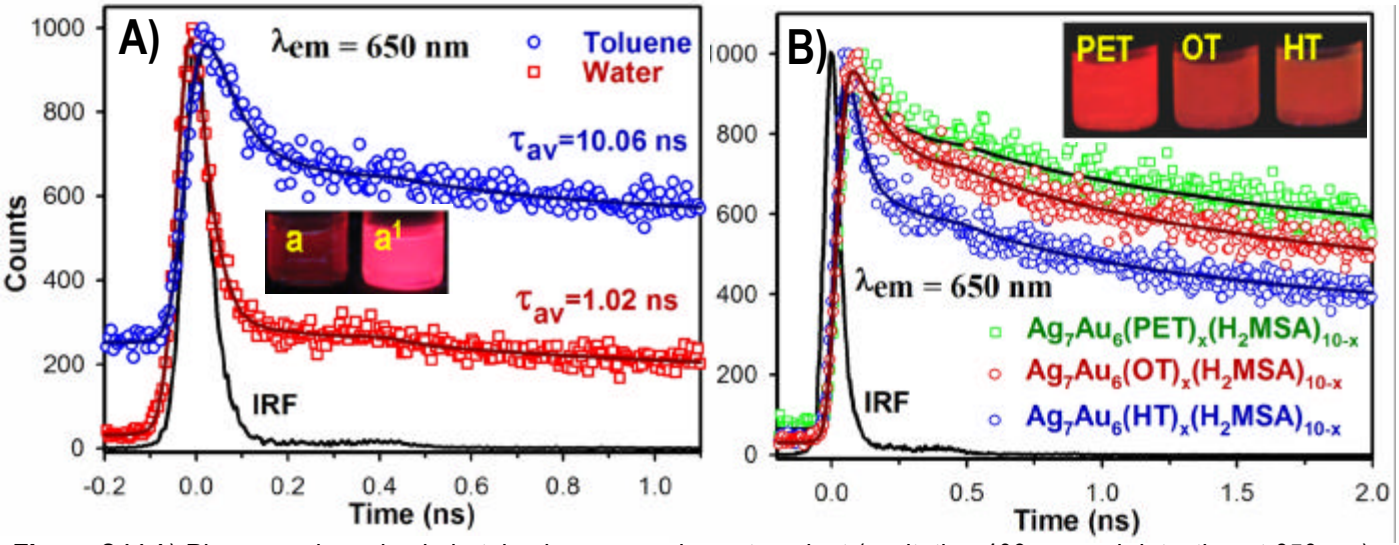

Figure S11 A) Picosecond resolved photoluminescence decay transient (excitation 409 nm and detection at 650 nm) of $Ag_7Au_6(H_2MSA)_{10}$ in aqueous solution and $Ag_7Au_6(H_2MSA)_{10}$ in toluene after phase transfer using tetraoctylammonium bromide. Both the decays are tri-exponential. Inset showing the photograph of the $Ag_7Au_6(H_2MSA)_{10}$ before (a) and after phase transfer (a^1). B) Photoluminescence decay transient (excitation 409 nm and detection at 650 nm) of $Ag_7Au_6(PET)_x(H_2MSA)_{10-x}$, $Ag_7Au_6(OT)_x(H_2MSA)_{10-x}$ and $Ag_7Au_6(HT)_x(H_2MSA)_{10-x}$. where PET-phenylethanethiol, HT- hexanethiol and OT- octanethiol. The numerical fitting and IRF are shown in solid lines. All the decay transients are tri-exponential. There seems to be a pattern of average lifetime which may depend on the electron donating property of the ligands. Picosecond resolved anisotropic studies would give more information. Inset shows the photographs of the $Ag_7Au_6(PET)_x(H_2MSA)_{10-x}$, $Ag_7Au_6(OT)_x(H_2MSA)_{10-X,}$ $Ag_7Au_6(HT)_x(H_2MSA)_{10-x}$ in toluene under UV light.

Table 1: Tabulated lifetime values of the $Ag_7Au_6(H_2MSA)_{10}$ cluster before and after phase transfer. Standard error in lifetime values is about 10%.

Solvent	Average lifetime(ns)	t_1(ns)	%	t_2(ns)	%	t_3(ns)	%
Water	1.0	0.02	93	1.2	3	25	4
Toluene	10.0	0.08	66	1.7	13	46	21

Table 2: Tabulated lifetime values of the ligand exchange products. Standard error in lifetime values is about 10%.

	Average lifetime (ns)	t_1(ns)	%	t_2(ns)	%	t_3(ns)	%
$Ag_7Au_6(PET)_x(H_2MSA)_{10-x}$	11.9	0.15	36	2.2	25	29	39
$Ag_7Au_6(OT)_x(H_2MSA)_{10-x}$	7.9	0.14	42	2.0	26	22	32
$Ag_7Au_6(HT)_x(H_2MSA)_{10-x}$	4.8	0.07	62	1.6	18	22	20

S13. Supporting information 13

TEM, SEM, EDAX, Optical images, Luminescence image of tubular arrangement of nanoparticles

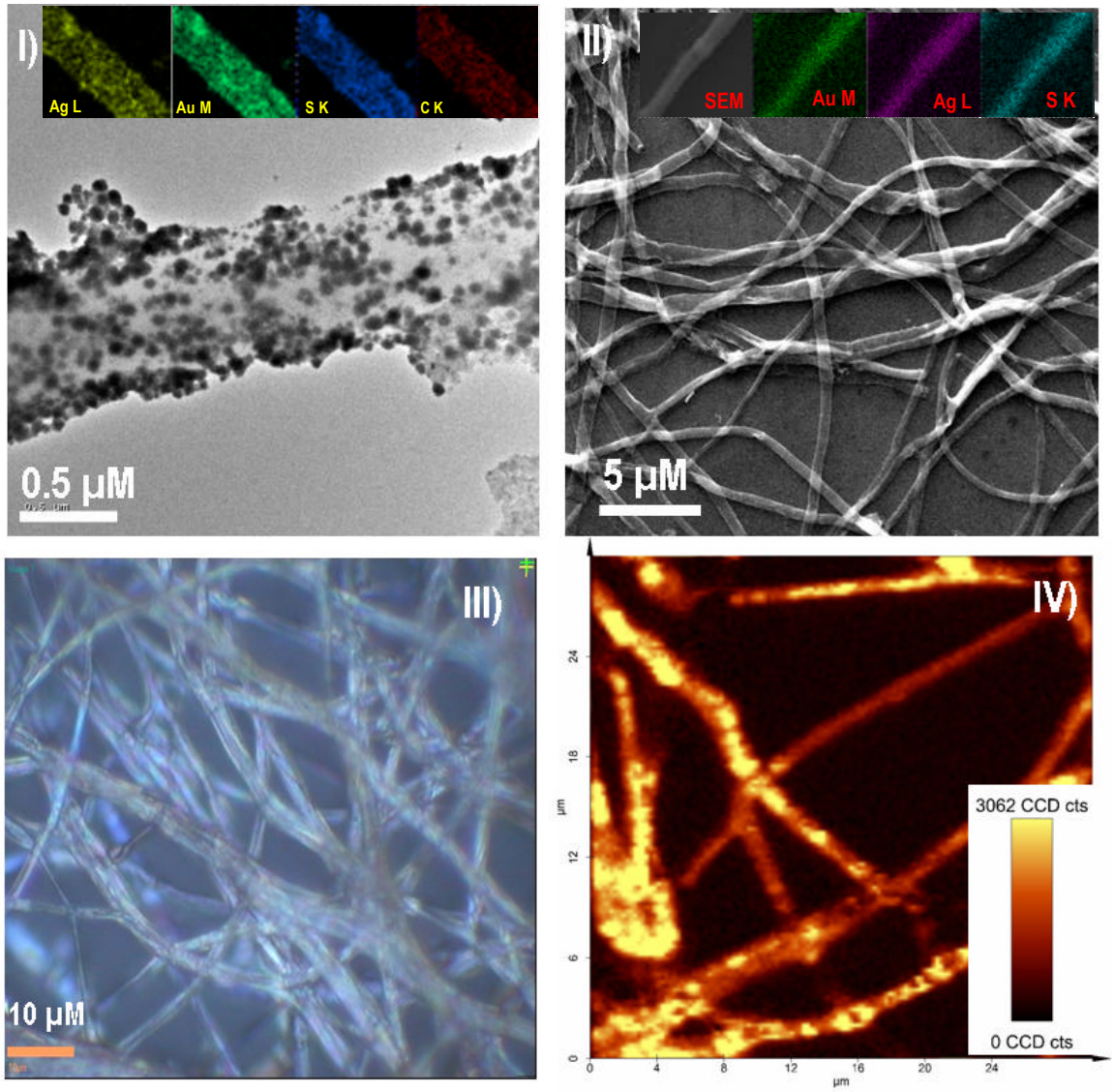

Figure S12. I) TEM images of the reaction product upon the addition of 500 µL of 10 mM $HAuCl_4$ to 100 µL crude silver cluster in 3 mL water. Note that here the amount of $HAuCl_4$ used is more than the optimized condition. Images show the presence of nanoparticles and their aggregation in a tubular manner where thiolate may be acting as a

template. Inset showing the TEM/EDAX maps of the reaction product were done using Au **M**$_a$, Ag **L**$_a$, S **K**$_a$ and C **K**$_a$. II) SEM images of the product showing the presence of the tubular structures. Inset showing the SEM image of one such tube on which the EDAX maps were done using Au **L**$_a$, Ag **M**$_a$ and S **K**$_a$. III) Optical image of the product showing the presence of the tubular structures. IV) Inherent solid state luminescence image of tubular structures collected by the spectroscopic mapping at an excitation wavelength of 532 nm. Regions coded bright yellow represents the pixels where the luminescence signal (used for mapping) is a maximum, the minima being represented with black. The scan area was 30 µm x 30 µm. Metallic nanoparticles are known to show this kind of luminescence background in Raman image.

S14. Supporting information 14

Optimizing the amount of (cluster: $HAuCl_4$)

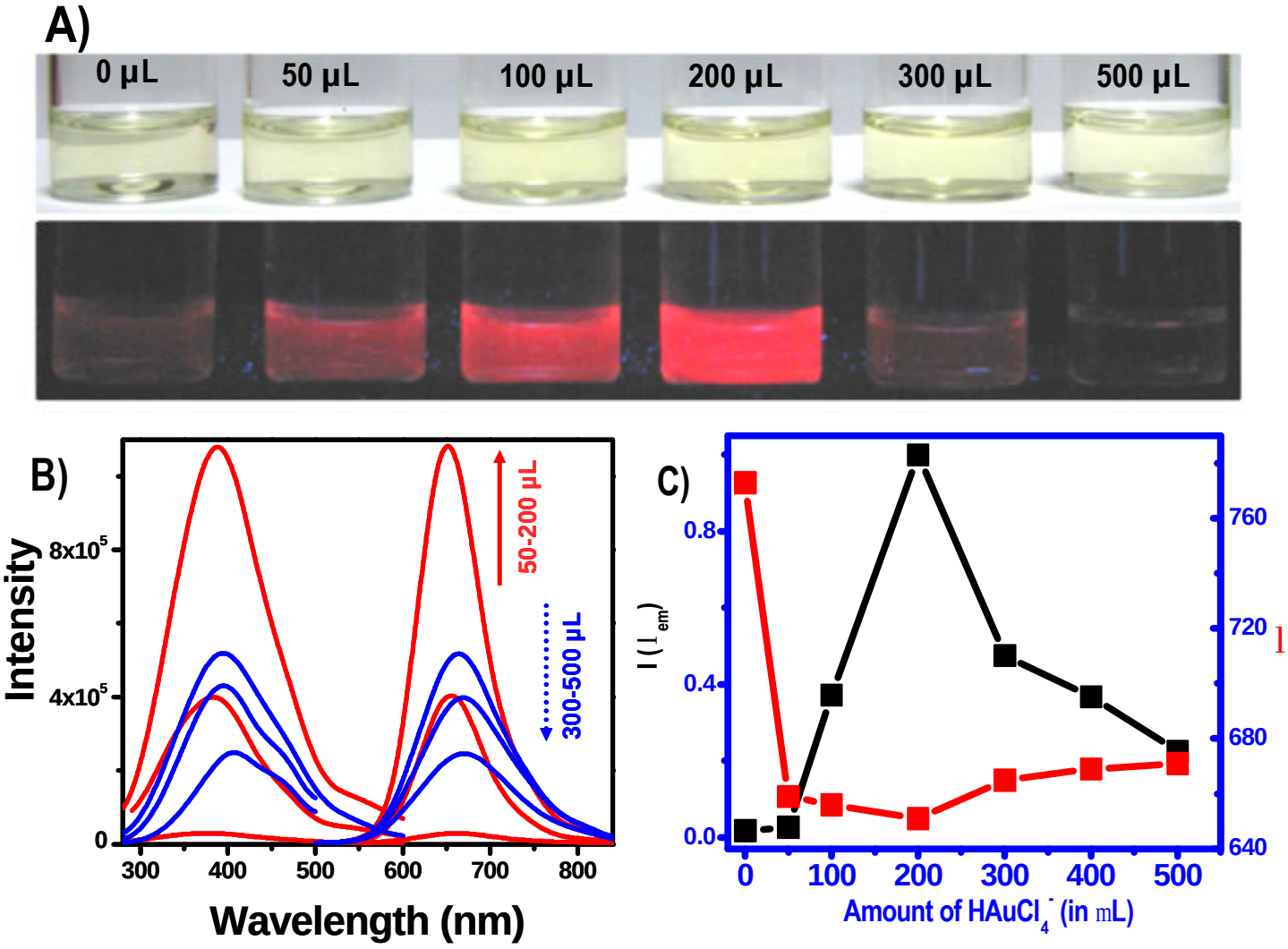

Figure S13.

A) Reactions at various amounts of 10 mM $HAuCl_4$ are photographed under white light and UV light. 100 µL of crude silver cluster solution was made-up to 3.0 mL distilled water. To these solutions, 50, 100, 200, 300, 400, 500 µL of 10 mM $HAuCl_4$ was added and stirred for 15 min at 293 K. Volume (3.0 mL) kept constant in all these cases. At these concentrations, solutions are very dilute and the color change was not observed under ambient light, whereas the cluster solutions photographed under UV light show a drastic change in the emission of each sample. Emission of crude silver cluster was very low at room temperature. Upon the

addition of $HAuCl_4$, emission got enhanced which was maximum for the addition 200 µL of $HAuCl_4$. Further addition leads to decreasing luminescence emission.

B) Changes in the luminescence emission profile during the addition of $HAuCl_4$ to the 100 µL of crude silver cluster in distilled water. Volume (3.0 mL) was constant in all these cases.

C) Changes in the luminescence emission position (?) and changes in the luminescence emission intensity [I($?_{em}$)] plotted against the amount of $HAuCl_4$. As-synthesized crude silver cluster showing luminescence emission at 770 nm which upon addition of 50, 100, 200, 300, 400, 500 µL of $HAuCl_4$ shifts to 650, 640, 630, 670, 675, 678 nm. Luminescence emission intensity was high for the reaction at 200 µL $HAuCl_4$. We used these concentrations for synthesizing larger amounts.

S15. Supporting information 15

Blank reactions

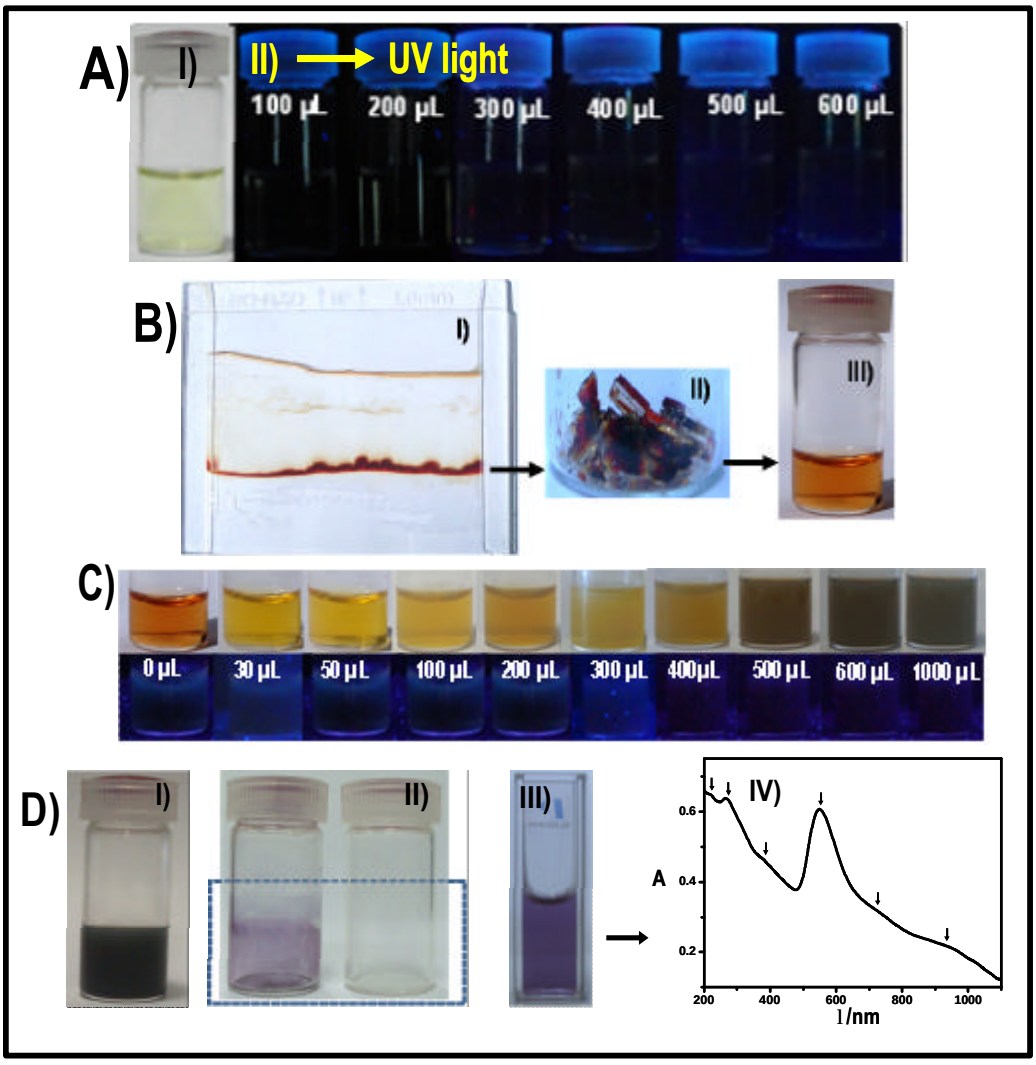

Figure S14.

A) Photograph of 3.0 mL of oligomeric siver thiolate solution taken in a bottle (I). To this solution, 50 to 600 µL of 10 mM $HAuCl_4$ was added and the photographs of the corresponding solutions under UV light are shown in (II). All of them do not show any luminescence. It is noted that in contrast, addition of $HAuCl_4$ to crude silver cluster shows bright luminescence. It shows that the reaction involved is not a simple silver complex- gold complex interaction.

B) (I) Photograph of the gel, containing Ag_8 cluster and selected portion of the band containing Ag_8 cluster was cut II). Cluster was extracted into distilled water whereas gel was insoluble. Pure Ag_8 solution is of golden brown color as shown in photograph III).

C) $HAuCl_4$ was added to the pure Ag_8 cluster in various amounts and allowed the reaction for 15 min at 300 K. Photographs of the cluster in visible and UV light are shown. Amounts of solution were not the same (gradual increase from left to right) due to the increase in the amount of addition of $HAuCl_4$. All of them are not showing any luminescence. This may be due to decomposition of Ag cluster and uncontrolled growth of gold after the nucleation step due to the lack of external stabilizing agent. Note that metallic nanoparticles exhibit very weak emission, not observable visibly.

D) I) Photograph of the reaction of pure Ag_8 and 1000 µL of $HAuCl_4$. II) After removal of the solution, deep blue layer appeared on the sides of the bottle which was very clear when it was compared with an empty bottle. III) Photograph of the deep blue layer which was readily dispersible in water. IV) UV-Vis spectrum of the solution showing various peaks. It is expected that these are from differently shaped nanoscale objects (see below). Various peaks are marked.

S16. Supporting information 16

TEM images of gold-silver nanomaterials

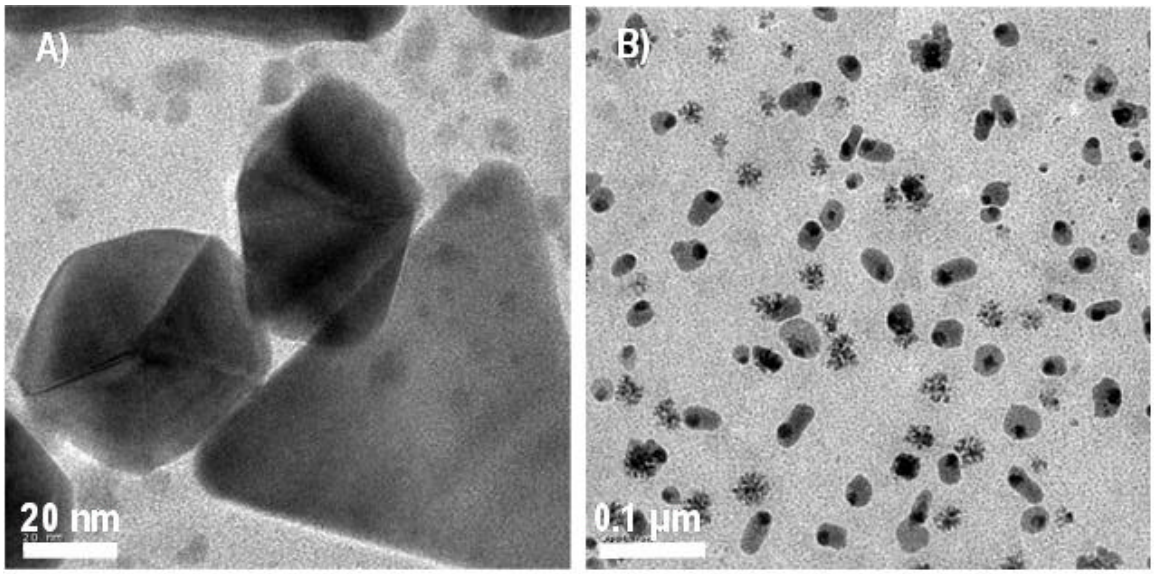

Figure S15. TEM images of the product obtained during the above mentioned reaction (S15 D, III, IV). A, B are the TEM images obtained from the same grid. 'A' shows the presence of decahedral gold nanoparticles and also gold triangles. 'B' shows the TEM images of various shaped silver-gold nanoscale objects.

S17. Supporting information 17

^{1}H NMR of $(Ag_mAu_n)_{QC}$@SG

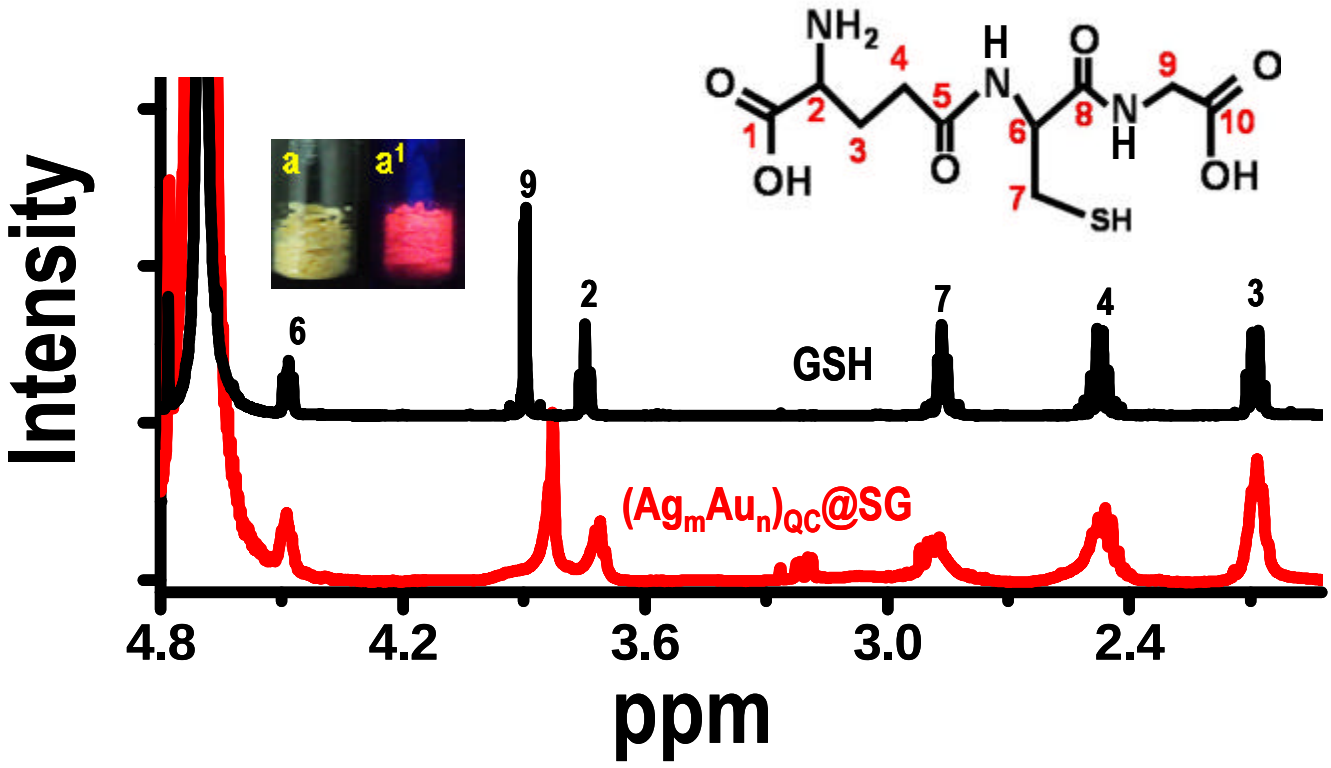

Figure S16. ^{1}H NMR of the $(Ag_mAu_n)_{QC}$@SG and glutathione(GSH). Peaks corresponding to the cluster become broader as compare to glutathione; especially H-7 (a-position) peak was more broadened and down field shifted due to the closer to cluster core. Inset showing the powder form of the sample collected in both visible (a) and UV light (a^1)

S18. Supporting information 18

Reactions of Au(I)MSA with $Ag_9(MSA)_7$ at various conditions

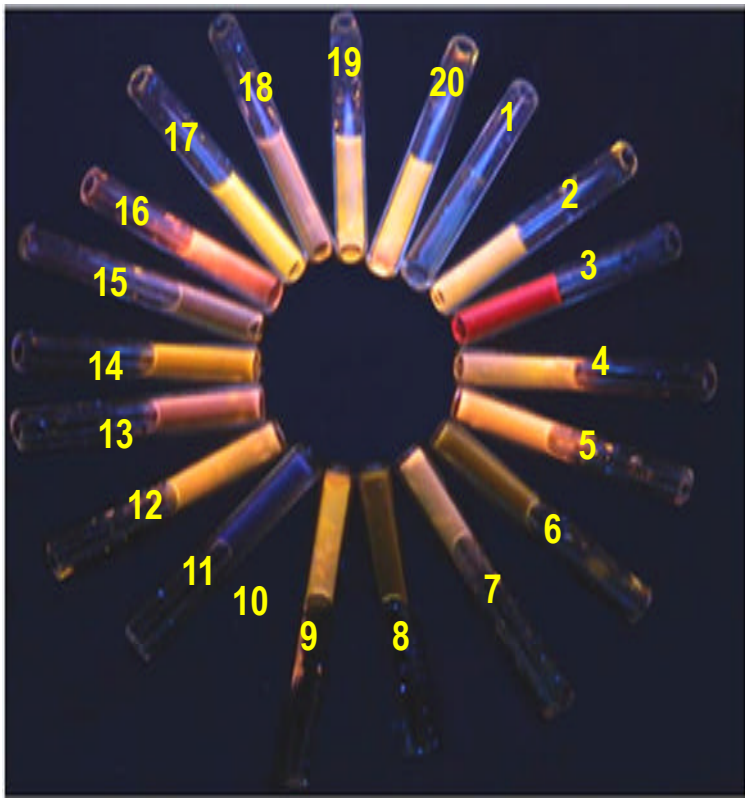

Figure S17. Photographs of the products of reaction between Au(I)MSA with $Ag_9(H_2MSA)_7$ at various Au(I)MSA concentrations keeping the concentration of $Ag_9(H_2MSA)_7$ the same. The photographs were taken under UV excitation. The glass sample vials were kept in a circular pattern. Image shows that alloy clusters of diverse composition and emission characteristics may be made by varying the experimental conditions.